Supplementary Material

SUPPLEMENTARY METHODS

1. The image processing and interpretation of DECT in diagnosis of uric acid stone

All patients underwent dual-energy CT (DECT) with a dual-source dual-energy SOMATOM Definition Flash machine (Siemens Healthcare, Forchheim, Germany). The patient was positioned supine on the CT table with an area of interest being the abdomen. Dual-energy scan was performed using the scanner which acquires the images at 100/140 kVp in two different planes by the two tubes of the machine angled at 90° to each other.

After the image acquisition, the dual energy dataset was subjected to preprogrammed dual energy algorithmic software and new datasets acquired which were analyzed by syngo.via software (Siemens Healthcare, Forchheim, Germany). The stone marker was located on the desired stone which revealed various dual energy parameters of the stone, such as HU values at 100/Sn140/fusion image and dual energy ratio, which were used to classify the stones into uric acid stones and non-uric acid stones. On the DECT images, uric acid stone is visualized as red, while non-uric acid stone is visualized as blue (prediction result). An example case is shown in the figures below.

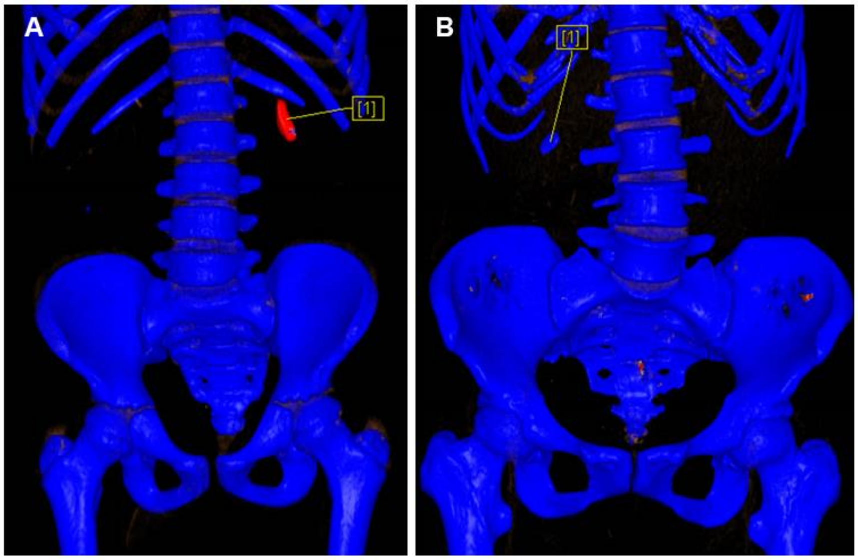

2. Detailed description of the LASSO algorithm

LASSO is a powerful method for regression with high dimensional predictors. In our study, the LASSO method was combined with a logistic regression model for analysis of the urinary stone types, which could select the most important predictive features from the training set. This method minimizes a log partial likelihood subject to the sum of the absolute values of the parameters being bounded by a constant:

$$\hat{\beta} = \operatorname{argmin} \ell(\beta), \text{ subject to } \sum\left|\beta_j\right| \leq s$$

where, $\hat{\beta}$ is the obtained parameters, $\ell(\beta)$ is the log partial likelihood of the logistic regression model, $s > 0$ is a constant.

The LASSO method can be used for feature reduction and selection by shrinking coefficients and forcing certain coefficients to be set to zero through absolute constraint [1]. In this study, the standardized constraint parameter s was set as 0.063, and 14 nonzero coefficients ($\hat{\beta}$) were selected by LASSO.

3. Decision curve analysis

In the study, the decision curve analysis (DCA) method was used to estimate the clinical usefulness of the presented radiomics model. The DCA algorithm evaluates prediction models by calculating the range of threshold probabilities in which a prediction or prognostic model is clinically useful. DCA is a comprehensive method for assessing and comparing different diagnostic and prognostic models. The theory of DCA can be illustrated by the equation below:

$$\frac{a-c}{d-b} = \frac{1-P_t}{P_t}$$

where d – b represents the influence of unnecessary treatment. If treatment is directed by a prediction model, d – b is the harm related to a false-positive result compared with a true-negative result. Inversely, a – c represents the consequence of rejecting beneficial treatment, in other words, the harm from a false-negative result compared with a true-positive result. Pt represents where the expected benefit of treatment is equal to the expected benefit of refraining from treatment [2, 3].

REFERENCES

1. Tibshirani R. Regression shrinkage and selection via the lasso: a retrospective. J R Stat Soc Series B Stat Methodol 2011; 73: 273-282. doi: 10.1111/j.1467-9868.2011.00771.x.
2. Balachandran VP, Gonen M, Smith JJ, DeMatteo RP. Nomograms in oncology: more than meets the eye. Lancet Oncol 2015; 16: e173-180. doi: 10.1016/s1470-2045(14)71116-7.
3. Vickers AJ, Elkin EB. Decision curve analysis: a novel method for evaluating prediction models. Med Decis Making 2006; 26: 565-574. doi: 10.1177/0272989x06295361.

SUPPLEMENTARY TABLES

Supplementary Table 1. The CT acquisition parameters.

	CT mode	Manufacturer	Tube voltage (kV)	Slice thickness (mm)
The First People's Hospital of Kashgar Prefecture	**Dual-energy CT**	SOMATOM Definition Flash (Siemens Healthcare, Germany)	100/140 (low/high tube voltage)	1.5
	Traditional non-contrast CT	GE Optima CT680 (GE Healthcare, USA)	110	1.25
		SOMATOM Emotion 16 eco (Siemens Healthcare, Germany)	110	1.5
Sun Yat-sen Memorial Hospital	**Traditional non-contrast CT**	GE Discovery CT750 HD (GE Healthcare, USA)	120	1.25
		SOMATOM Sensation 64 eco (Siemens Healthcare, Germany)	120	1.0

Supplementary Table 2. Extracted radiomics features.

Group	Subgroup	Radiomics Features
First-order statistics features		Interquartile Range, Skewness, Uniformity, Median, Energy, Robust Mean Absolute Deviation, Mean Absolute Deviation, Total Energy, Maximum, Root Mean Squared, 90th Percentile, Minimum, Entropy, Range, Variance, 10th Percentile, Kurtosis, Mean
Shape-based features		Voxel Volume, Mesh Volume, Surface Volume Ratio, Maximum 3D Diameter, Maximum 2D Diameter Slice, Sphericity, Minor Axis, Elongation, Major Axis, Surface Area, Flatness, Least Axis, Maximum 2D Diameter Column, Maximum 2D Diameter Row
Statistics-based textural features	GLCM	Joint Average, Sum Average, Joint Entropy, Cluster Shade, Maximum Probability, Inverse Difference Moment Normalized, Joint Energy, Contrast, Difference Entropy, Inverse Variance, Difference Variance, Inverse Difference Normalized, Inverse Difference Moment, Correlation, Autocorrelation, Sum Entropy, Maximal Correlation Coefficient, Sum Squares, Cluster Prominence, Informal Measure of Correlation 2, Informal Measure of Correlation 1, Difference Average, Inverse Difference, Cluster Tendency
	GLRLM	Short Run Low Gray Level Emphasis, Gray Level Variance, Low Gray Level Run Emphasis, Gray Level Non-Uniformity Normalized, Run Variance, Gray Level Non-Uniformity, Long Run Emphasis, Short Run High Gray Level Emphasis, Run Length Non-Uniformity, Short Run Emphasis, Long Run High Gray Level Emphasis, Run Percentage, Long Run Low Gray Level Emphasis, Run Entropy, High Gray Level Run Emphasis, Run Length Non-Uniformity Normalized
	GLSZM	Gray Level Variance, Zone Variance, Gray Level Non-Uniformity Normalized, Size Zone Non-Uniformity Normalized, Size Zone Non-Uniformity, Gray Level Non-Uniformity, Large Area Emphasis, Small Area High Gray Level Emphasis, Zone Percentage, Large Area Low Gray Level Emphasis, Large Area High Gray Level Emphasis, High Gray Level Zone Emphasis, Small Area Emphasis, Low Gray Level Zone Emphasis, Zone Entropy, Small Area Low Gray Level Emphasis
	GLDM	Gray Level Variance, High Gray Level Emphasis, Dependence Entropy, Dependence Non-Uniformity, Gray Level Non-Uniformity, Small Dependence Emphasis, Small Dependence High Gray Level Emphasis, Dependence Non-Uniformity Normalized, Large Dependence Emphasis, Large Dependence Low Gray Level Emphasis, Dependence Variance, Large Dependence High Gray Level Emphasis, Small Dependence Low Gray Level Emphasis, Low Gray Level Emphasis
	NGTDM	Coarseness, Complexity, Strength, Contrast, Business
Wavelet features*†		wavelet(LLL)_x, wavelet(LLH)_x, wavelet(LHL)_x, wavelet(LHH)_x, wavelet(HLL)_x, wavelet(HLH)_x, wavelet(HHL)_x, wavelet(HHH)_x
LoG filtered features*‡		LoG(σ=1)_x, LoG(σ=2)_x, LoG(σ=3)_x, LoG(σ=4)_x

* x denotes the first-order statistics features and statistics-based textural features listed above.

† For the wavelet filter, each image was filtered using either a high-bandpass filter or a low-bandpass filter in the x, y, and z directions, yielding 8 different combinations of decompositions. The value in brackets indicates the filters (H: High-pass filter, L: Low-pass filter) applied in the x, y, and z directions.

‡ For the LoG filter, images were filtered using a 3D LoG filter implemented in SimpleITK and by changing sigma values to 4.0, 3.0, 2.0, and 1.0 mm, yielding another 4 derived images. The value in brackets indicates the filter width used for the Gaussian kernel.

Detailed information about the feature names and mathematical formulas can be obtained from the *pyradiomics* documentation available at http://pyradiomics.readthedocs.io/en/latest.

Abbreviations: LoG: Laplacian of Gaussian; GLCM: Gray Level Cooccurence Matrix; GLRLM: Gray Level Run Length Matrix; GLSZM: Gray Level Size Zone Matrix; GLDM: Gray Level Dependence Matrix; NGTDM, neighboring gray tone difference matrix.

Supplementary Table 3. R packages used in our study.

Statistical analysis	R package
LASSO logistic regression	glmnet
ROC curves	pROC
Logistic regression, nomogram construction, and calibration plot	rms
Collinearity diagnosis	car
Hosmer-Lemeshow test	vcdExtra
Decision curve analysis	dca.R
Net reclassification improvement (NRI) and integrated discrimination improvement (IDI)	nricens PredictABEL

Supplementary Table 4. Baseline characteristics of the patients who underwent dual-energy CT.

Characteristic	
Age, years	
Median (Interquartile range)	27 (19, 42)
Sex	
Male	135 (75.8)
Female	43 (24.2)
Number of stones	
Single	38 (21.3)
Multiple	140 (78.7)
Stone location	
Kidney	148 (83.2)
Ureter	23 (12.9)
Bladder or Urethra	7 (3.9)
Stone composition	
Uric acid	30 (16.9)
Ammonium urate	21 (11.8)
Calcium oxalate	127 (71.3)
DECT diagnosis result	
Uric acid	41 (23.0)
Non-uric acid	137 (77.0)

Data are presented as No. (%) unless indicated otherwise.

Supplementary Table 5. Baseline characteristics of the patients used for model construction and validation.

Characteristic	Training set (n = 93)	Internal validation set (n = 40)	External validation set (n = 109)
Age, years			
Median (Interquartile range)	32 [17, 49]	38.5 [21, 56]	56 [49, 66]
Sex			
Male	65 (70)	30 (75)	67 (61.5)
Female	28 (30)	10 (25)	42 (38.5)
Number of stones			
Single	35 (38)	14 (35)	23 (21.1)
Multiple	58 (62)	26 (65)	86 (78.9)
Stone location			
Kidney	70 (75)	29 (73)	82 (75.2)
Ureter	12 (13)	6 (15)	17 (15.6)
Bladder or Urethra	11 (12)	5 (12)	10 (9.2)
Urine white blood cell count			
< 100 per µl	36 (39)	18 (45)	65 (59.6)
≥ 100 per µl	57 (61)	22 (55)	44 (40.4)
Urine nitrite			
Negative	67 (72)	30 (75)	101 (92.7)
Positive	26 (28)	10 (25)	8 (7.3)
Urine pH			
Median (Interquartile range)	5.5 [5.5, 6.0]	5.5 [5.0, 6.0]	5.5 [5.5, 6.0]
Urine culture			
Positive	27 (29)	5 (13)	14 (12.8)
Negative	66 (71)	35 (87)	95 (87.2)
Stone composition			
Ammonium urate	47 (51)	17 (43)	20 (18.3)
Uric acid	46 (49)	23 (57)	89 (81.7)

Data are presented as No. (%) unless indicated otherwise.

Supplementary Table 6. Stratified analysis of the association between the radiomics signature and stone types in all enrolled patients.

	Subgroups	Radiomics score		*Z*	*P*
		Ammonium urate stones	**Uric acid stones**		
Sex	Male	-0.860 (-1.019, -0.252)	1.310 (0.728, 2.043)	-8.872	< 0.001
	Female	-0.394 (-1.060, 0.098)	1.474 (0.675, 1.858)	-5.380	< 0.001
Stone location	Kidney	-0.623 (-0.997, -0.062)	1.372 (0.708, 1.972)	-8.638	< 0.001
	Ureter	-0.950 (-1.463, -0.184)	1.236 (0.650, 1.665)	-4.193	< 0.001
	Bladder or Urethra	-0.998 (-1.030, -0.955)	1.737 (1.061, 2.062)	-4.015	< 0.001
Number of stones	Single	-0.678 (-1.064, -0.267)	1.300 (0.736, 1.882)	-6.750	< 0.001
	Multiple	-0.691 (-1.007, -0.029)	1.372 (0.525, 1.980)	-7.870	< 0.001
Urine white blood cell count	< 100	-0.610 (-1.186, -0.010)	1.483 (0.734, 2.029)	-5.081	< 0.001
	≥ 100	-0.743 (-1.014, -0.166)	1.300 (0.461, 1.765)	-7.847	< 0.001
Urine nitrite	Negative	-0.684 (-1.008, -0.145)	1.431 (0.752, 1.974)	-8.898	< 0.001
	Positive	-0.674 (-1.066, -0.109)	0.592 (-0.164, 1.680)	-4.106	< 0.001
Urine culture	Negative	-0.802 (-1.141, -0.187)	1.337 (0.722, 1.964)	-8.989	< 0.001
	Positive	-0.411 (-0.891, -0.062)	1.391 (0.003, 2.007)	-4.354	< 0.001

Radiomics scores are shown as medians (interquartile ranges).

Z and *P* values were derived from the Mann–Whitney *U* tests.

SUPPLEMENTARY FIGURES

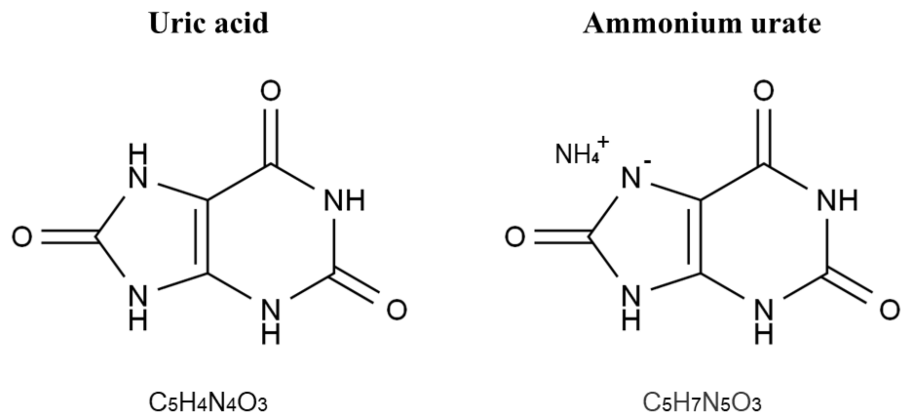

Supplementary Figure 1. The chemical structural formulas of uric acid and ammonium urate.

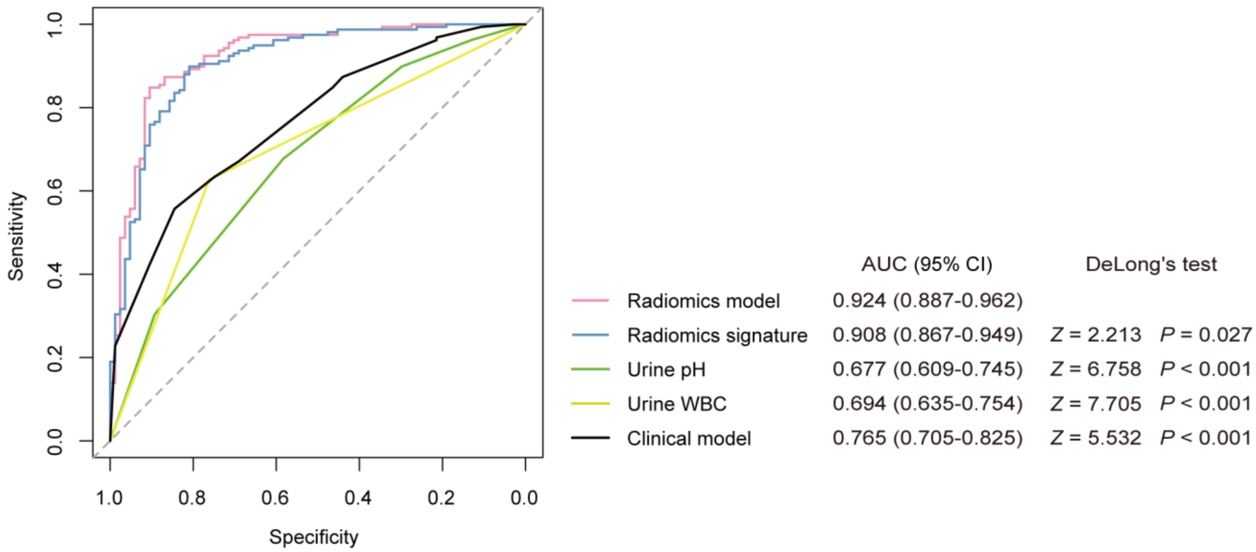

Supplementary Figure 2. Model comparisons using ROC curve analyses.

ROC curves comparing the predictive performance of the radiomics model with each selected predictor and the clinical model in all enrolled patients.

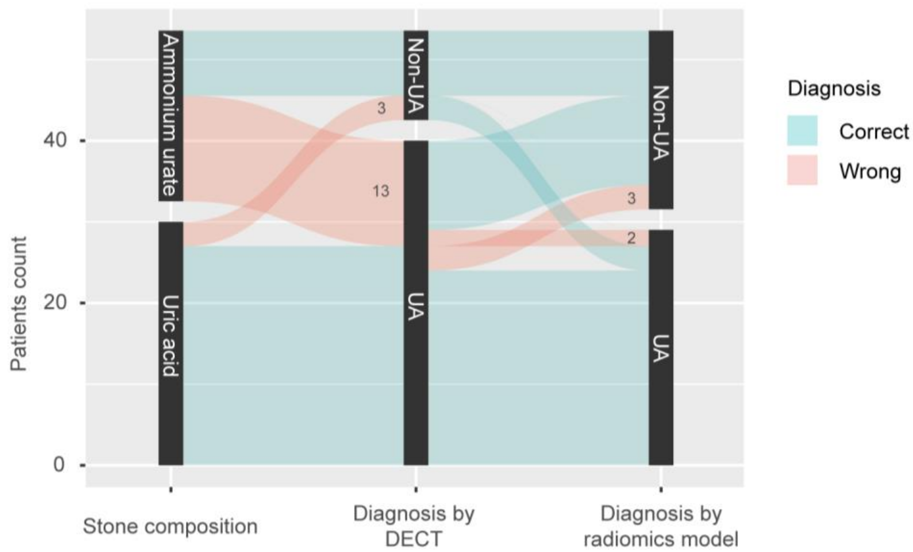

Supplementary Figure 3. Sankey diagram presents the reclassification of patients diagnosed by DECT and the radiomics model.

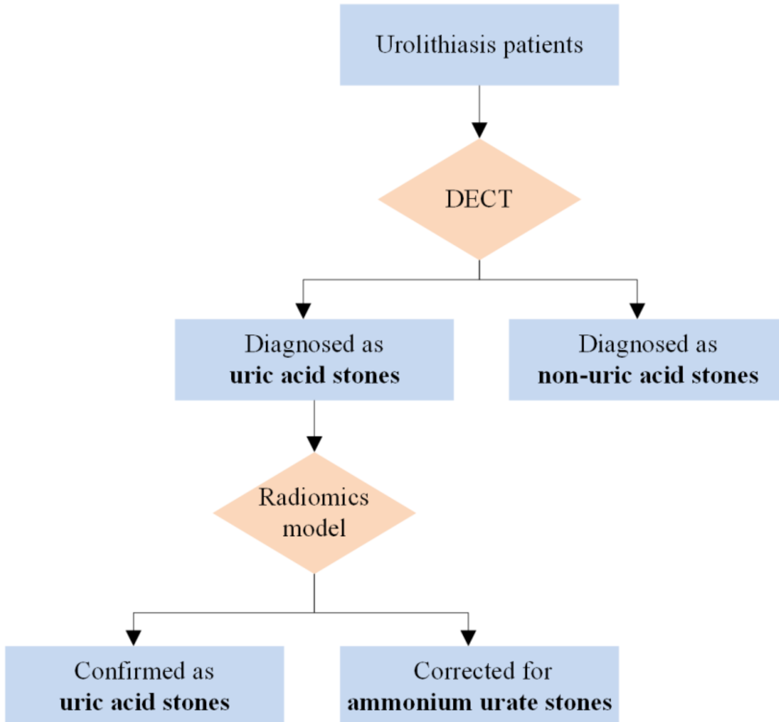

Supplementary Figure 4. The recommended diagnostic workflow for the individualized use of our proposed radiomics model.